Cannabis yield, potency, and leaf photosynthesis respond differently to increasing light levels in an indoor environment

Victoria Rodriguez Morrison[†], David Llewellyn[†], and Youbin Zheng[*]

School of environmental Sciences, University of Guelph, Guelph, Ontario, Canada, N1G 2W1

* Correspondence:
Youbin Zheng
yzheng@uoguelph.ca

Abstract

Since the recent legalization of medical and recreational use of cannabis (*Cannabis sativa* L.) in many regions worldwide, there has been high demand for research to improve yield and quality. With the paucity of scientific literature on the topic, this study investigated the relationships between light intensity (LI) and photosynthesis, inflorescence yield, and inflorescence quality of cannabis grown in an indoor environment. After growing vegetatively for 2 weeks under a canopy-level photosynthetic photon flux density (PPFD) of ≈ 425 $\mu mol \cdot m^{-2} \cdot s^{-1}$ and an 18-h light/6-h dark photoperiod, plants were grown for 12 weeks in a 12-h light/12-h dark 'flowering' photoperiod under canopy-level PPFDs ranging from 120 to 1800 $\mu mol \cdot m^{-2} \cdot s^{-1}$ provided by light emitting diodes. Leaf light response curves varied both with localized (i.e., leaf-level) PPFD and temporally, throughout the flowering cycle. Therefore, it was concluded that the leaf light response is not a reliable predictor of whole-plant responses to LI, particularly crop yield. This may be especially evident given that dry inflorescence yield increased linearly with increasing canopy-level PPFD up to 1800 $\mu mol \cdot m^{-2} \cdot s^{-1}$, while leaf-level photosynthesis saturated well below 1800 $\mu mol \cdot m^{-2} \cdot s^{-1}$. The density of the apical inflorescence and harvest index also increased linearly with increasing LI, resulting in higher-quality marketable tissues and less superfluous tissue to dispose of. There were no LI treatment effects on cannabinoid potency, while there were minor LI treatment effects on terpene potency. Commercial cannabis growers can use these light response models to determine the optimum LI for their production environment to achieve the best economic return; balancing input costs with the commercial value of their cannabis products.

1   INTRODUCTION

Drug-type *Cannabis sativa* L. (hereafter, cannabis) is often produced indoors to allow complete control of environmental conditions, which is important for producing consistent medicinal plants and products (United Nations Office on Drugs and Crime, 2019; Zheng, 2020). Total reliance on electrical lighting for plant production gives growers the capability to manipulate crop morphology, yield, and quality using light. However, lighting-related costs comprise $\approx 60\%$ of total energy used for indoor cannabis production (Evergreen Economics, 2016; Mills, 2012); making crop lighting one of the most substantial input costs for growing cannabis indoors. With recent nationwide legalization in Canada (among many other regions worldwide), energy demand for indoor cannabis production is expected to increase rapidly as the industry intensifies production to address rising demand (Sen and Wyonch, 2018).

41   There are many factors that govern the cost of producing photosynthetically active radiation (PAR)
42   for indoor cannabis production. These factors include: the capital and maintenance costs of lighting
43   fixtures and related infrastructure, efficiency of converting electricity into PAR (usually referred to as
44   PAR efficacy; in units of $\mu mol_{(PAR)} \cdot J^{-1}$), management of excess heat and humidity, and uniformity of
45   PAR distribution within the plant canopy. The most common lighting technologies used for indoor
46   cannabis production are high intensity discharge (e.g., high pressure sodium) and light emitting
47   diodes (LED). These technologies have widely varying spectrum, distribution, PAR efficacy, and
48   capital costs. However, regardless of the lighting technology used, the dominant factor that regulates
49   the cost of crop lighting is the target canopy-level light intensity (LI).

50   One common precept in controlled-environment agriculture production is that crop yield responds
51   proportionally to increasing LI; i.e. the so-called "1% rule" whereby 1% more PAR equals 1%
52   greater yield (Marcelis et al., 2006). On a per-leaf basis, this principle is clearly limited to lower light
53   intensities, since light use efficiency (i.e., maximum quantum yield; QY, $\mu mol_{(CO_2)} \cdot \mu mol^{-1}_{(PAR)}$) of
54   all photosynthetic tissues begins to decline at LI well below their light saturation points (LSP; i.e.,
55   the LI at peak photosynthetic rate) (Posada et al., 2012). However, in indoor-grown cannabis, it is
56   conceivable that whole-plant photosynthesis will be maximized when LI at the upper canopy leaves
57   are near their LSP. This is partly attributable to the inter-canopy attenuation of PAR from self-
58   shading; allowing lower-canopy foliage to function within the range of LIs where their respective
59   LUE are optimized (Terashima and Hikosaka, 1995). This may be especially relevant to indoor
60   production, where relatively small changes in distance from the light source can impart substantial
61   differences in foliar LI (Niinemets and Keenan, 2012). Further, distinguished from many other
62   indoor-grown crops, cannabis foliage appears to tolerate very high LI, even when exposed to
63   photosynthetic photon flux densities (PPFD) that are much higher than what they have been
64   acclimated to (Chandra et al., 2015).

65   There is a paucity of peer-reviewed studies that have related LI to cannabis potency and yield (e.g.,
66   mass of dry, mature inflorescence per unit area and time). Perhaps the most referenced studies
67   reported aspects of single-leaf photosynthesis of several cultivars and under various PPFD, CO_2
68   concentration, and temperature regimes (Chandra et al., 2011; 2015; Lydon et al., 1987). These
69   works have demonstrated that cannabis leaves have very high photosynthetic capacity. However,
70   they have limited use in modeling whole canopy photosynthesis or predicting yield because single-
71   leaf photosynthesis is highly variable; depending on many factors during plant growth such as: leaf
72   age, their localized growing environments (e.g., temperature, CO_2, and lighting history), and
73   ontogenetic stage (Bauerle et al., 2020; Carvalho et al., 2015; Murchie et al., 2002; Zheng et al.,
74   2006). While lighting vendors have long relied on cannabis leaf photosynthesis studies to sell more
75   light fixtures to cannabis growers, their models are only tangentially related to whole-canopy
76   photosynthesis, growth, and (ultimately) yield (Kirschbaum, 2011).

77   Some forensic studies have utilized various methods to develop models to estimate crop yield from
78   illicit indoor cannabis production (Backer et al., 2019; Potter and Duncombe, 2012; Toonen et al.,
79   2006; Vanhove et al., 2011). These models used an array of input parameters (e.g., planting density,
80   growing area, crop nutrition factors, etc.) but, they relied on "installed wattage" (i.e., $W \cdot m^{-2}$) as a
81   proxy for LI. It is notable that reporting yield as $g \cdot W^{-1}$ (i.e., $g \cdot m^{-2} / W \cdot m^{-2}$) overlooks the
82   instantaneous time factor inherent in power units (i.e., $W = J \cdot s^{-1}$). A more appropriate yield metric
83   would also account for the length of the total lighting time throughout the production period (i.e., $h \cdot d^{-1} \times d$), thus factoring out the time units resulting in yield per unit energy input (e.g., $g \cdot kWh^{-1}$).
85   Further, area-integrated power does not directly correlate to the canopy-level light environment due

86   to myriad unknowns, such as hang height, light distribution, and fixture efficacy. It is therefore
87   impossible to accurately ascertain canopy-level LI in these models. Eaves et al. (2020) reported linear
88   relationships between canopy-level LI (up to 1500 µmol·m^{-2}·s^{-1}) and yield; however, they had only
89   one LI treatment above 1000 µmol·m^{-2}·s^{-1}. Further, they reported substantial inter-repetition
90   variability in their yield models, which indicates that factors other than LI may have limited crop
91   productivity in some circumstances. While methodological deficiencies in these studies may limit the
92   confident quantitative extrapolation of their results to production environments, it is striking that
93   none of these studies reported evidence of saturation of inflorescence yield at very high LI.

94   These studies all demonstrate the exceptionally high capacity that cannabis has for converting PAR
95   into biomass. However, there are also clear knowledge gaps in cannabis' photosynthesis and yield
96   responses to increasing LI. Further, cannabis products are very high-value commodities relative to
97   other crops grown in indoor environments. This means that producers may be willing to accept
98   substantially higher lighting-related input costs in order to promote higher yields in limited growing
99   areas. However, maximizing yield regardless of cost is not a feasible business model for most
100   cannabis producers; rather there is a trade-off between input costs and crop productivity by selecting
101   the optimum canopy-level LI (among other inputs) that will maximize net profits. Further
102   complicating matters, producers must balance fixed costs which do not vary with crop productivity
103   (such as property tax, lease rates, building security, and maintenance, etc.) and variable costs (such as
104   the aforementioned lighting-related costs among other crop inputs) which can have dramatic impacts
105   on crop productivity and yield (Vanhove et al., 2014). Since indoor crop lighting is a compromise
106   between input costs and crop productivity, it is critical for growers to select the optimum light
107   intensity (LI) for their respective production environment and business models.

108   The objectives of this study were to establish the relationships between canopy-level LI, leaf-level
109   photosynthesis, and yield and quality of drug-type cannabis. We investigated how plant growth stage
110   and localized foliar PPFD (LPPFD; i.e., instantaneous PPFD at leaf-level) affected photosynthetic
111   parameters and leaf morphology, and how growing cannabis at average canopy-level PPFDs
112   (APPFD; i.e., lighting history) ranging from 120 to 1800 µmol·m^{-2}·s^{-1} affected plant morphology,
113   yield, and quality of mature marketable inflorescence. The results of this study will assist the indoor
114   cannabis industry to determine how much PAR cannabis growers should be providing to the crop
115   canopy in order to maximize profits while minimizing energy use within their specific production
116   scenarios.

2   MATERIAL AND METHODS

118   The trial area consisted of 2 adjacent deep-water culture basins (CB) located in an indoor cannabis
119   production facility in Southern Ontario, Canada. Each CB (14.6 x 2.4 m) consisted of 24 parallel
120   polystyrene rafts (0.6 x 2.4 m), each containing holes for 16 plant pots, oriented in 2 rows with 30-cm
121   spacing both within- and between-rows. This spacing provided for 384 plants to be evenly spaced
122   within each CB, at a density of 0.09 m^2/plant.

123   Above each CB were 3 racks of LED fixtures (Pro-650; Lumigrow, Emeryville, CA, USA), with
124   each rack consisting 2 rows of 4 fixtures each; arranged such that all 24 fixtures were uniformly-
125   spaced (1.2 m apart, on-center) relative to each other and centered over the footprint of the CB. Each
126   rack of fixtures was height-adjustable via a system of pulleys and cables, such that the hang-height of
127   the 8 fixtures in each rack could be adjusted in unison. Each fixture contained dimmable spectrum
128   channels for blue (B, peak 455 nm), white (broad-spectrum 5000K) and red (R, peak 660 nm) which

3

129   could be individually controlled, wirelessly, through Lumigrow's SmartPAR software. The photon
130   flux ratio of B (400-500 nm), green (G, 500-600 nm), and R (600-700 nm) was B18:G5:R77.
131   Relative spectral photon flux distribution (**Figure 1**) was measured using a radiometrically calibrated
132   spectrometer (UV-VIS Flame-S-XR; Ocean Optics, Dunedin, FL, USA) coupled to a CC3 cosine-
133   corrector attached to a 1.9 m x 400 µm UV-Vis optical fibre.
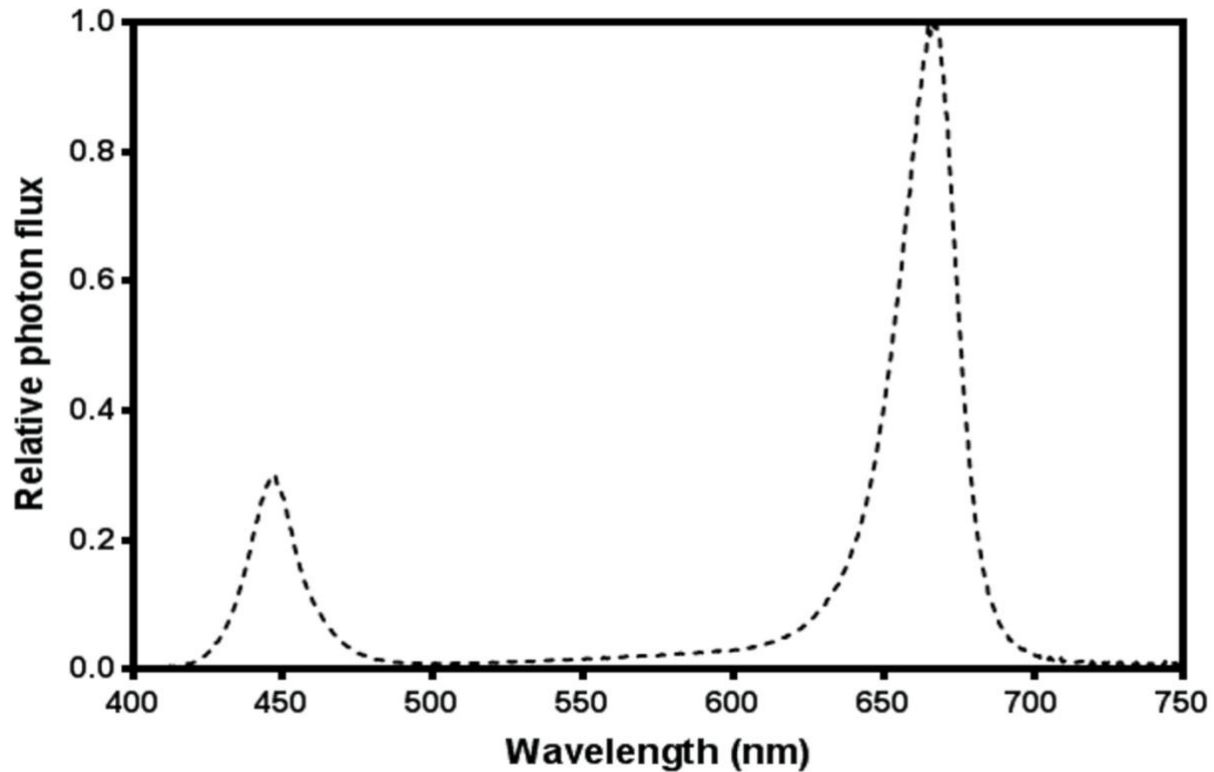
135   **Figure 1.** Relative spectral photon flux distribution of Pro-650 (Lumigrow) light-emitting diode
136   (LED) fixtures.

137   **2.1   Experimental Design**

138   The experiment was conducted using a gradient design, whereby plants grown in a common
139   environment were exposed to a broad range of canopy-level PPFDs with a high level of spatial
140   variability across the CB. Individual plants were assigned $_APPFD$ levels based on rigorous spatial
141   and temporal evaluations of LI (explained below). Gradient designs can outperform traditional
142   "treatment x replication" experimental designs when evaluating plants' responses to a continuous
143   variable such as LI (Kreyling et al., 2018). While they are arduous to setup and monitor, gradient
144   designs have been successfully used to establish LI effects within other controlled-environment
145   production scenarios (Bredmose, 1993, 1994; Jones-Baumgardt et al., 2019).

146   At its outset, the experiment was arranged as a randomized complete block design (RCBD) with 6
147   blocks of 8 PPFD target levels: 200, 400, 600, 800, 1000, 1200, 1400, and 1600 µmol·m^{-2}·s^{-1}, to
148   facilitate setup. Each block consisted of a single rack of LED fixtures, with the PPFD target levels
149   randomly assigned to individual fixtures (i.e., plots) within each rack. The two plants located most
150   directly below each fixture were assessed experimentally. PPFD was measured at the apex of each

4

151 plant using a portable spectroradiometer (LI-180; LI-COR Biosciences, Lincoln, NE, USA). The
152 initial hang height of each rack was determined by the maximum height whereby approximately 1600
153 $\mu mol \cdot m^{-2} \cdot s^{-1}$ could be achieved at the apical meristem of the tallest plant in the highest LI plot. The
154 other treatment levels were subsequently achieved through dimming; targeting the prescribed PPFD
155 at the apical meristem of the tallest plant in each plot while maintaining a uniform photon flux ratio
156 of B18:G5:R77 in the entire CB. Plant height and apical meristematic PPFD were measured twice
157 weekly until vegetative growth ceased (five weeks after the start of the 12-h photoperiod), and
158 weekly thereafter until harvest. The prescribed intensity levels in each block were reset each time
159 plant height was measured, first by raising the rack of fixtures to achieve the target PPFD at the
160 apical meristem of the tallest plant in the 1600 $\mu mol \cdot m^{-2} \cdot s^{-1}$ plot and then adjusting the intensity
161 settings of the remaining plots accordingly. The trial ran from the beginning of the flowering stage
162 (i.e., when the 12-h flowering photoperiod was initiated) until harvest, for a total of 81 days (nearly
163 12 weeks).

164 While the underlying experimental arrangement was based on a RCBD organization, all analyses
165 were performed as regressions with LI as the continuous, independent variable.

2.2 PPFD Levels

167 While the prescribed target PPFD levels were maintained at the apical meristem at the tallest plant
168 within each plot on regular intervals, these values were not accurate proxies for the actual PPFD
169 intensity dynamics experienced by each plant throughout the trial due to variability in individual
170 plant height (on intra- and inter-plot bases), growth rates, and the lengths of the time periods between
171 PPFD measurements. To account for these temporal dynamics in apical meristematic PPFD, total
172 light integrals (TLIs, $mol \cdot m^{-2}$) were calculated for each plant over the total production time and then
173 back-calculated to APPFD or daily light integral (DLI, $mol \cdot m^{-2} \cdot d^{-1}$). The TLIs were based on the
174 product of the average PPFD level measured at the start and end of each measurement interval and
175 the length of time the lights were on during each measurement interval. These interim light integrals
176 were then aggregated to form a TLI for each plant and divided by the total production time in
177 seconds (i.e., the product of the daily photoperiod and the number of days). The resulting APPFD
178 levels were then used as the independent variable (i.e., X-axis) in regressions of LI vs. various
179 growth, yield and quality parameters. TLI can also be used in yield evaluations whereby the
180 relationship between yield and TLI becomes a direct measure of production efficacy on a quantum
181 basis (e.g., $g \cdot mol^{-1}$). This relationship can be converted to an energy-basis ($g \cdot kWh^{-1}$), if the fixture
182 efficacy ($\mu mol \cdot J^{-1}$) and spatial distribution efficiency (i.e., proportion of photon output from fixtures
183 that reach the target growing area) are known.

2.3 Plant Culture

185 Cuttings were taken from mother plants of the 'Stillwater' cultivar on 1 Aug. and 15 Aug. 2019 and
186 rooted in stone wool cubes under 100 $\mu mol \cdot m^{-2} \cdot s^{-1}$ of fluorescent light for 14 d and then transplanted
187 into a peat-based medium in 1-gallon plastic pots and grown under $\approx$ 425 $\mu mol \cdot m^{-2} \cdot s^{-1}$ of LED light,
188 comprised of a mixture of Pro-325 (Lumigrow) and generic phosphor-converted white LEDs
189 (unbranded) for an additional 14 d. The apical meristems were removed (i.e., "topped") from the first
190 batch of clones, 10 d after transplant, and the second batch were not topped. Propagation and
191 vegetative growth phases both had 18-h photoperiods. The first CB (CB1) was populated from the
192 first batch of clones on 29 Aug. 2019 and the second CB (CB2) was populated from the second batch
193 of clones on 12 Sept. 2019. In each case, 48 uniform and representative plants were selected from the
194 larger populations of clones and placed in the plots to be evaluated experimentally. In CB1, the

5

195   experimental plants initially had either 9 or 10 nodes and ranged in height (from growing medium
196   surface to shoot apex) from 34 to 48 cm. In CB2 the experimental plants initially had either 12 or 13
197   nodes and ranged in height from 41 to 65 cm. Once the plants were moved to the CBs, the daily
198   photoperiod switched to 12 h, from 06:30 HR to 18:30 HR.

199   Plant husbandry followed the cultivator's standard operating procedures except for the differences in
200   canopy-level PPFD. Canopy-level air temperature, relative humidity (RH), and carbon dioxide (CO_2)
201   concentration were monitored on 600-s intervals throughout the trial with a logger (Green Eye model
202   7788; AZ Instrument Corporation, Taiwan). The air temperature, RH, and CO_2 concentrations were
203   (mean ± SD) 25.3 ± 0.4 °C, 60.5 ± 4.8%, and 437 ± 39 ppm during the day (i.e., lights on) and 25.2 ±
204   0.3 °C, 53.1 ± 3.3%, and 479 ± 42 ppm during the night. A common nutrient solution is circulated
205   through both CBs. The nutrient concentrations in the aquaponic solution were sampled weekly and
206   analyzed at an independent laboratory (A&L Canada; London, ON, Canada). The nutrient element
207   concentrations ($mg \cdot L^{-1}$) in the aquaponic system were (mean ± SD, n = 11): 170 ± 22 Ca, 86 ± 8.2 S,
208   75 ± 15 N, 57 ± 5 Mg, 32 ± 4 P, 23 ± 8 K, 250 ± 32 Cl, 0.27 ± 0.1 Fe, 0.18 ± 0.07 Zn, 0.050 ± 0.02
209   Mn, 0.031 ± 0.006 B, and 0.028 ± 0.004 Cu. Mo was reported as below detection limit (i.e., < 0.02
210    $mg \cdot L^{-1}$) throughout the trial. The concentrations ($mg \cdot L^{-1}$) of non-essential nutrient elements were 170
211   ± 18 Na and 6.7 ± 0.7 Si. The aquaponic solution was aerated with an oxygen concentrator and the
212   pH and EC were 6.75 ± 0.2 and 1.77 ± 0.15 $mS \cdot cm^{-1}$, respectively.

2.4   Leaf Photosynthesis

214   Quantifications of leaf-level gas exchange of leaflets on the youngest, fully-expanded fan leaves were
215   performed on 64 plants (32 plants per CB) each, in weeks 1, 5, and 9 after the initiation of the 12-h
216   photoperiod using a portable photosynthesis machine (LI-6400XT; LI-COR Biosciences), equipped
217   with the B and R LED light source (6400-02B, LI-COR Biosciences). The Light Curve Auto-
218   Response subroutine was used to measure net carbon exchange rate (NCER; $\mu mol_{(CO_2)} \cdot m^{-2} \cdot s^{-1}$) at
219   PPFD levels of: 2000, 1600, 1400, 1200, 1000, 800, 600, 400, 200, 150, 100, 75, 50, 25, and 0
220    $\mu mol \cdot m^{-2} \cdot s^{-1}$. Leaflets were exposed to 2000 $\mu mol \cdot m^{-2} \cdot s^{-1}$ for 180 s prior to starting each light
221   response curve (LRC) and then progressed sequentially from highest to lowest PPFD to ensure
222   stomatal opening was not a limitation of photosynthesis (Singsaas et al., 2001). The leaf chamber
223   setpoints were 26.7°C (block temperature), 400 ppm CO_2, and 500 $\mu mol \cdot s^{-1}$ airflow. The localized
224   PPFD (LPPFD) at each leaflet was measured immediately prior to the LRC measurement using the
225   LI-180. The light-saturated net CO_2 exchange rate (A_{sat}; $\mu mol_{(CO_2)} \cdot m^{-2} \cdot s^{-1}$), localized NCER
226   (LNCER; i.e., the NCER at LPPFD), maximum quantum yield (QY; $\mu mol_{(CO_2)} \cdot \mu mol^{-1}_{(PAR)}$), and
227   light saturation point (LSP; $\mu mol_{(PAR)} \cdot m^{-2} \cdot s^{-1}$) were determined for each measured leaflet using
228   Prism (Version 6.01; GraphPad Software, San Diego, CA, USA) with the asymptotic LRC model: y
229   = a + b·$e^{(c \cdot x)}$ (Delgado et al., 1993) where y, x, a, and *e* represent NCER, PPFD, A_{sat}, and Euler's
230   number, respectively. The LNCER of each leaflet was calculated by substituting the measured
231   LPPFD into its respective LRC model. The QY was calculated as the slope of the linear portion of the
232   LRC (i.e., at PPFD ≤ 200 $\mu mol \cdot m^{-2} \cdot s^{-1}$). The LSP is defined as the PPFD level where increasing LI
233   no longer invokes a significant increase in NCER. The LSP for each LRC was determined using the
234   methods described by Lobo et al. (2013) by evaluating the change in NCER (ΔNCER) over 50
235    $\mu mol_{(PAR)} \cdot m^{-2} \cdot s^{-1}$ increments, continuously along the LRC, until the ΔNCER reached a threshold
236   value, which was determined from the prescribed measurement conditions and performance
237   specifications of the LI-6400XT. Briefly, the minimum significant difference in CO_2 concentration
238   between sample and reference measurements is 0.4 ppm (LI-COR Biosciences, 2012). Therefore,

6

239   given the setup parameters of the leaf chamber, a ΔNCER of ≤ 0.33 $\mu mol_{(CO_2)} \cdot m^{-2} \cdot s^{-1}$ over a 50
240    $\mu mol_{(PAR)} \cdot m^{-2} \cdot s^{-1}$ increment indicated the LSP.

241   The ratio of variable to maximum fluorescence (F_v/F_m) emitted from photosystem II (PSII) in dark-
242   acclimated leaves exposed to a light-saturating pulse is an indicator of maximum quantum yield of
243   PSII photochemistry (Murchie and Lawson, 2013). Immediately after each LRC, the leaflet was dark
244   acclimated for ≈ 900 s and then F_v/F_m was measured with a fluorometer (FluorPen FP 100; Drasov,
245   Czech Republic). Chlorophyll content index (CCI) was measured on three fan leaflets from leaves at
246   the bottom and top of each plant in weeks 1, 5, and 9 using a chlorophyll meter (CCM-200; Opti-
247   Sciences, Hudson, NH, USA). The CCI measurements from upper and lower tissues, respectively,
248   were averaged on a per-plant basis for each measurement period.

2.5   Leaf Morphology

250   On day 35, one leaf from each plant was removed from node 13 (counting upwards from the lowest
251   node) in CB1 and node 15 from CB2, ensuring that the excised leaves developed under their
252   respective LPPFD. A digital image of each leaf was taken using a scanner (CanoScan LiDE 25;
253   Canon Canada Inc., Brampton, ON, Canada) at 600 dpi resolution and then the leaves were oven-
254   dried (Isotemp Oven Model 655G; Fisher Scientific, East Lyme, CT, USA), singly, to constant
255   weight at 65°C. The images were processed using ImageJ 1.42 software (National Institute of Health;
256   https://imagej.nih.gov/ij/download.html) to determine leaf area (LA). The dry weights (DW) of
257   scanned leaves were measured using an analytical balance (MS304TS/A00; Mettler-Toledo,
258   Columbus, OH, USA). Specific leaf weight (SLW; $g \cdot m^{-2}$) was determined using the following
259   formula: DW / LA.

2.6   Yield and Quality

261   After 81 d, the stems of each plant was cut at substrate level and the aboveground biomass of each
262   plant was separated into three parts: apical inflorescence, remaining inflorescence, and stems and
263   leaves (i.e., non-marketable biomass), and weighed using a digital scale (Scout SPX2201; OHAUS
264   Corporation, Parsippany, NJ, USA). Since the plants from CB2 had the apical meristem removed, the
265   inflorescence from the tallest side branch was considered the apical inflorescence. The length (L) and
266   circumference (C; measured at the midpoint) of each apical inflorescence were also measured.
267   Assuming a cylindrical shape, the density of the apical inflorescence (AID, $g \cdot cm^{-3}$) was calculated
268   using the formula: AID = fresh weight/$\{\pi \cdot [C/(2 \cdot \pi)^2] \cdot L\}$. The apical inflorescences from 22
269   representative plants from CB1 were air dried at 15 °C and 40% RH for 10 d until they reached
270   marketable weight (i.e., average moisture content of $\approx 11\%$), determined using a moisture content
271   analyzer (HC-103 Halogen Moisture Analyzer; Mettler-Toledo, Columbus, OH, USA). This ensured
272   that the apical inflorescence tissues selected for analysis of secondary metabolites followed the
273   cultivator's typical post-harvest treatment. The apical inflorescences from CB1 were homogenized on
274   a per-plant basis and ≈ 2-g sub-samples from each plant was processed by an independent laboratory
275   (RPC Science & Engineering; Fredericton, NB, Canada) for potency ($mg \cdot g^{-1}_{(DW)}$) of 11 cannabinoids
276   and 22 terpenes using ultra-high-performance liquid chromatography and mass spectrometry. Total
277   equivalent Δ-9-tetrahydrocannabinol (Δ^9-THC), cannabidiol (CBD), and cannabigerol potencies were
278   determined by assuming complete carboxylation of the acid-forms of the respective cannabinoids,
279   whose concentrations were adjusted by factoring out the acid-moiety from the molecular weight of
280   each compound [e.g., total Δ^9-THC = (Δ^9-THCA x 0.877) + Δ^9-THC]. The separated aboveground
281   tissues from 16 representative plants in each CB were oven-dried (Isotemp Oven Model 655G) to

282 constant weight at 65°C to determine LI treatment effects on moisture content, which were then used
283 to determine DW of all harvested materials. The harvest index (HI) was calculated as the ratio of
284 total inflorescence DW (hereafter, yield) to the total aboveground DW, on a per-plant basis.

285 **2.7   Data Processing and Analysis**

286 On per-CB and per-week bases, each model from the leaf photosynthesis measurements (i.e., A_{sat},
287 LSP, LNCER, and QY) were subjected to non-linear regression using the PROC NLMIXED
288 procedure (SAS Studio Release 3.8; SAS Institute Inc., Cary, NC), with the LPPFD of each measured
289 leaf as the independent variable, to determine the best-fit models after outliers were removed. In
290 each case, best-fit models were selected based on the lowest value for the Akaike information
291 criterion (AICc). If there were no LI treatment effects on a given parameter, then means ($\pm$ SD) were
292 calculated. Best-fit models for F_v/F_m and CCI were similarly determined, using LPPFD and APPFD
293 (from the start of the trial up to the time of measurement), respectively, as the independent variable.
294 On a per-week basis, A_{sat}, LSP, LNCER, QY, F_v/F_m, and CCI data from CB1 and CB2 were pooled if
295 the 95% confidence intervals (95% CI) of each element of the respective best-fit models for the two
296 CBs overlapped, and best-fit models for pooled datasets were then recalculated. The PROC
297 GLIMMIX Tukey-Kramer test was used ($P \le 0.05$) on the resulting models (including means) to
298 determine if there were differences between the measurement periods (i.e., weeks). If there were any
299 measurement period effects on any element in the models, then weekly models for the respective
300 parameters were reported.

301 Computed parameters from single-time measurements (SLW, AID, yield, and HI) were grouped per
302 CB, using the APPFD (at the time of measurement) to define each datapoint within each CB and
303 PROC NLMIXED was used to evaluate the best fit model for each parameter using the AICc.
304 Parameter means were computed (on per-CB bases) when there were no LI treatment effects. If there
305 were LI treatment effects on a given parameter, datasets from CB1 and CB2 were pooled if the 95%
306 confidence intervals (95% CI) of each element of the respective best-fit models for the two CBs
307 overlapped and best-fit models for pooled datasets were then recalculated. For parameters with no LI
308 treatment effects, differences between CBs were evaluated using the 95% CI's of their respective
309 means. For a given parameter, if the 95% CIs the parameter means for the 2 CBs overlapped, then the
310 data was pooled and new parameter means were calculated and presented. Cannabinoids and terpenes
311 from CB1 were modeled, with APPFD as the independent variable, using PROC NLMIXED to
312 evaluate the best-fit model for each parameter using the AICc. Best-fit models or parameter means
313 were reported.

314 **3   RESULTS**

315 No CB effects were found in any leaf photosynthesis, leaf morphology, and post-harvest parameters;
316 therefore, CB1 and CB2 data were pooled for the development of all models except secondary
317 metabolites, which were only measured in CB1. In contrast, many of the parameters that were
318 repeated over time (i.e., in weeks 1, 5, and 9) showed differences between weeks; whereby the
319 different weeks were modeled separately. Note also that the week-over-week ranges of LPPFD varied
320 as the plants progressed through their ontogeny, since self-shading from upper tissues resulted in
321 decreases in maximum LPPFD of leaves selected for photosynthesis measurements. Nevertheless, a

322   consistent range of APPFDs range was maintained throughout the trial.
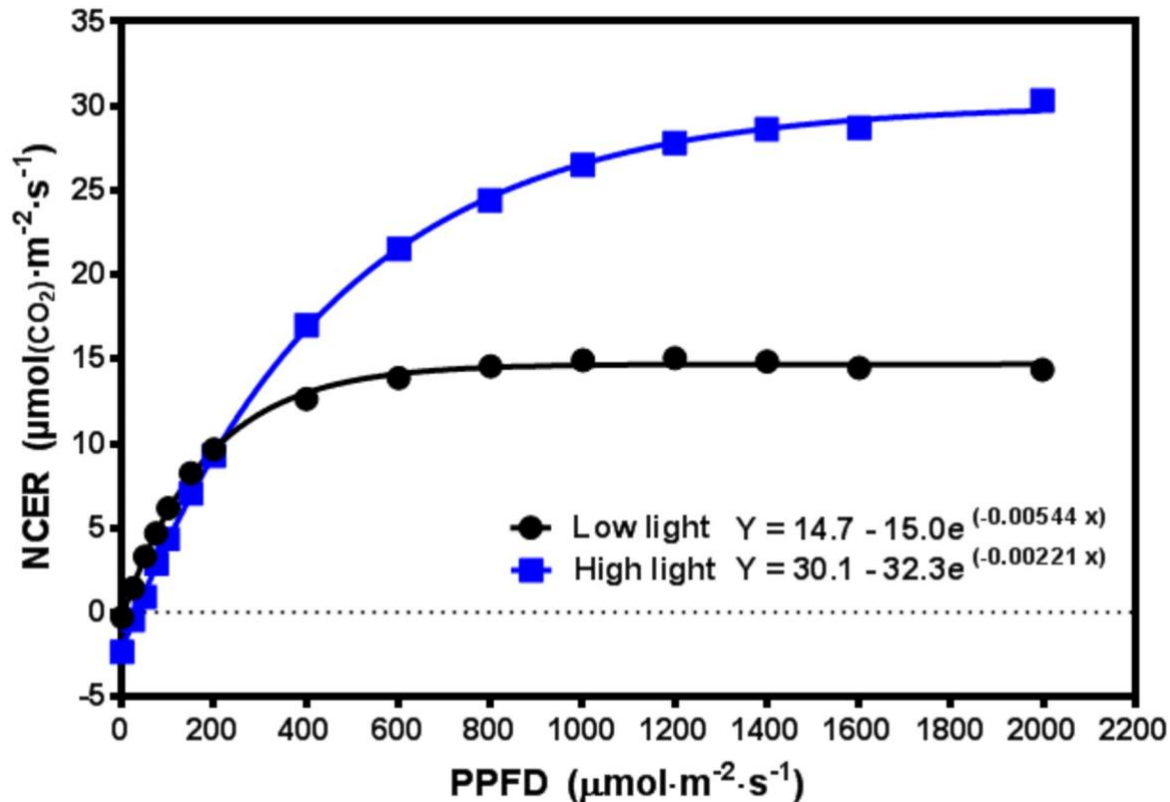
323

324   **Figure 2.** Typical light response curves [net CO_2 exchange rate (NCER) response to light intensity]
325   of the youngest fully-expanded fan leaves of *Cannabis sativa* L. 'Stillwater' grown under either low
326   or high localized photosynthetic photon flux densities (LPPFD). The low and high LPPFD were 91
327   and 1238 $\mu mol \cdot m^{-2} \cdot s^{-1}$, respectively. Measurements were made during week 5 after the initiation of
328   the 12-h photoperiod.
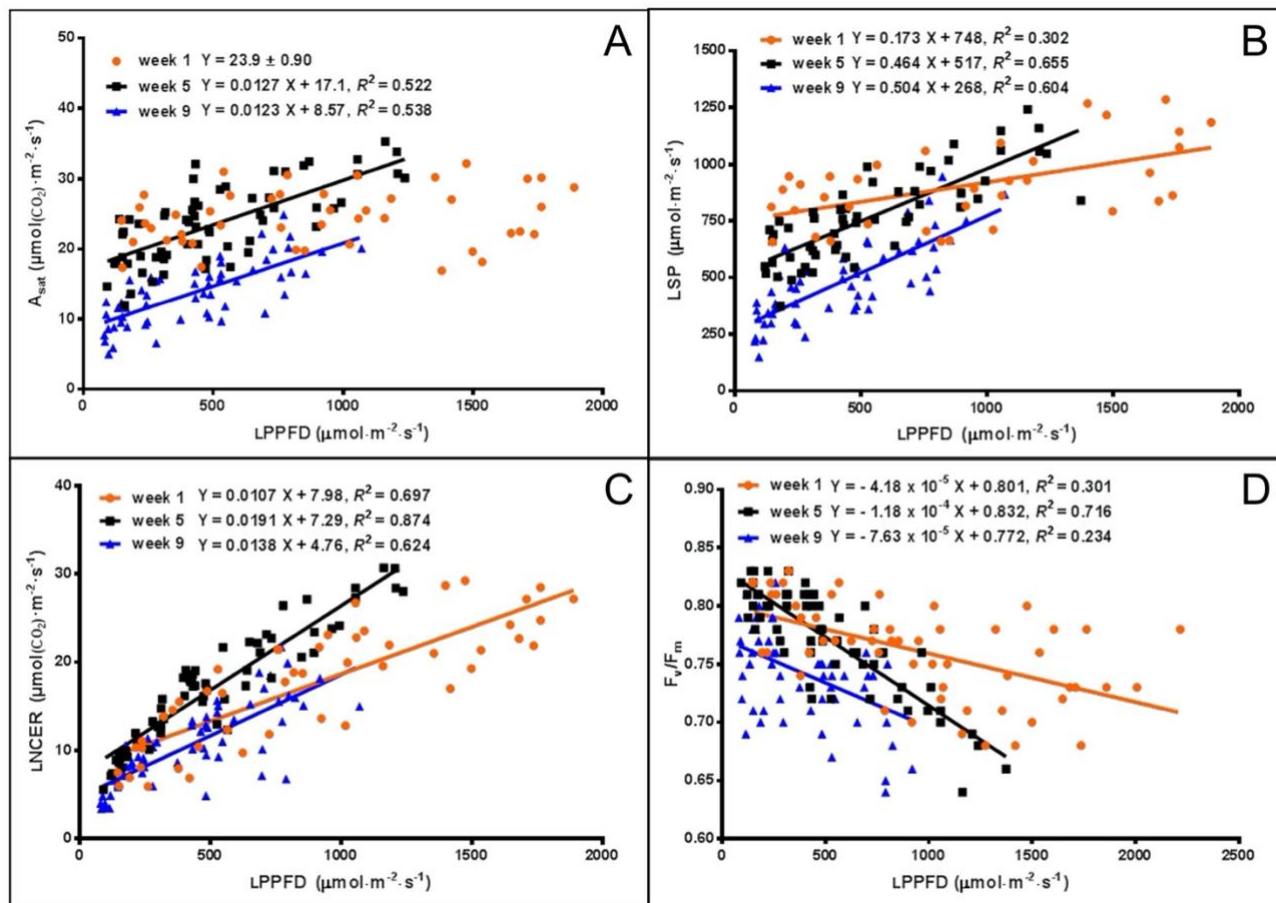
Figure 3. The light-saturated net CO_2 exchange rate (A_{sat}) **(A)**, the light saturation point (LSP) **(B)**, the localized net CO_2 exchange rate (LNCER) **(C)**, and the F_v/F_m **(D)** of the youngest fully-expanded fan leaves of *Cannabis sativa* L. 'Stillwater' at the localized photosynthetic photon flux densities (LPPFD) that the respective leaves were growing under when the measurements were made, during weeks 1, 5, and 9 after initiation of the 12-h photoperiod. Each datum is a single plant. Regression lines are presented when $P \leq 0.05$.

3.1 Leaf Photosynthesis

Leaf light response curves constructed under different LI and at different growth stages (week 1, 5, and 9) generally demonstrated the trends that the A_{sat} and LSP were higher for plants grown under high vs. low LPPFD (**Figures 2, 3A-B**), especially after the plants had acclimated to their new lighting environments (i.e., weeks 5 and 9). There were no LPPFD effects on A_{sat} in week 1, with a mean ($\pm$ SE, n = 52) of 23.9 ± 0.90 $\mu mol_{(CO_2)} \cdot m^{-2} \cdot s^{-1}$ (**Figure 3A**). The A_{sat} in weeks 5 and 9 (**Figure 3A**) and LSP in weeks 1, 5, and 9 (**Figure 3B**) increased linearly with increasing LPPFD. At low LPPFD, the highest LSP was in week 1. The slopes of the A_{sat} and LSP models were similar in weeks 5 and 9, but the Y-intercepts for both parameters were approximately twice as high in week 5 vs. week 9. LNCER increased linearly with increasing LPPFD in weeks 1, 5, and 9 (**Figure 3C**) with the steepest and shallowest slopes coming in weeks 5 and 1, respectively. The LNCER model in week 9 had a substantially lower Y-intercept than the other two weeks. As evidenced by the projected

10

349   intersection of the A_{sat} and LNCER models in week 5 (i.e., at LPPFD of 1532 $\mu mol \cdot m^{-2} \cdot s^{-1}$), the
350   maximum LPPFD in week 5 (i.e., 1370 $\mu mol \cdot m^{-2} \cdot s^{-1}$) was nearly sufficient to saturate the
351   photosynthetic apparatus at the top of the canopy. There were no LPPFD effects on QY, but the mean
352   QY in weeks 1 and 5 were higher than week 9. The mean ($\pm$ SE) QY were 0.066 ± 0.0013 (n = 54),
353   0.068 ± 0.0005 (n = 60), and 0.058 ± 0.0008 (n = 63) $\mu mol_{(CO_2)} \cdot \mu mol^{-1}_{(PAR)}$ in weeks 1, 5, and 9
354   respectively. The F_v/F_m decreased linearly with increasing LPPFD in all three measurement periods
355   (**Figure 3D**). The F_v/F_m model from week 5 had the largest Y-intercept (0.832) but also the steepest
356   slope.
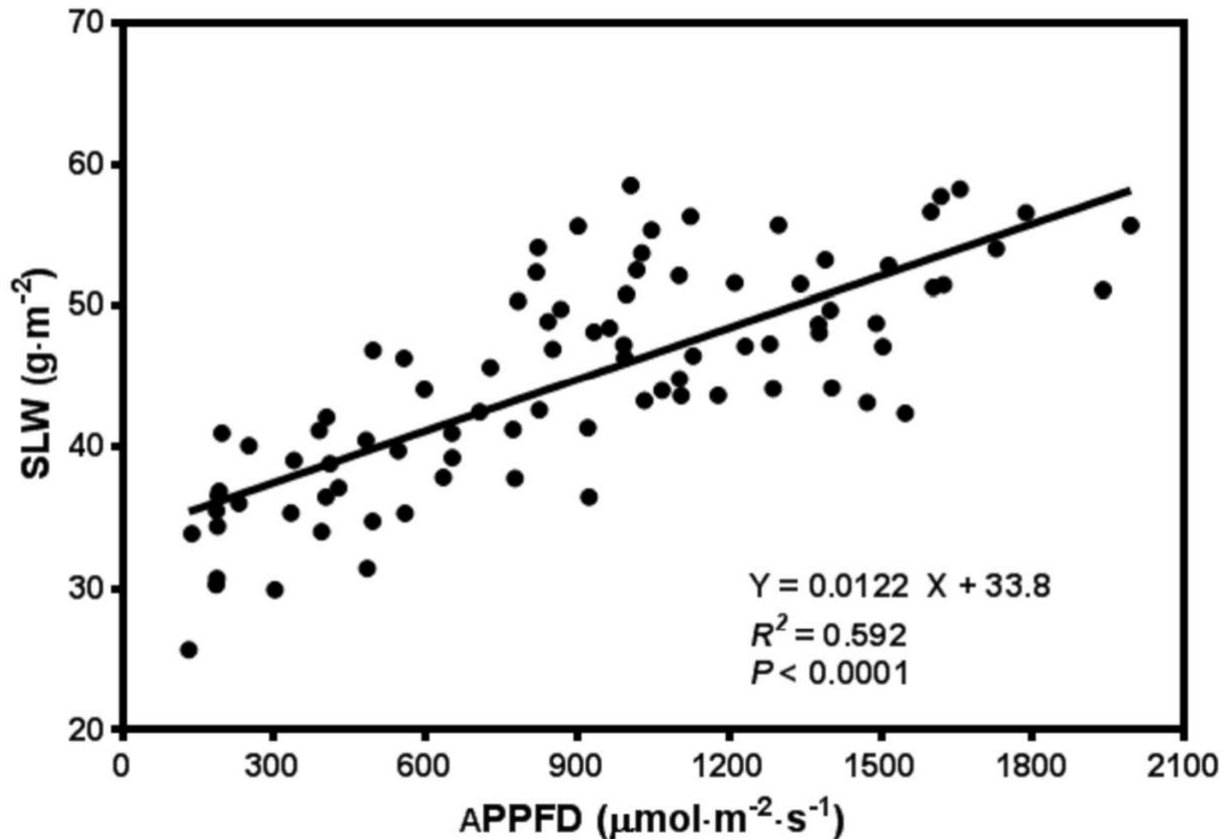
357

358   **Figure 4.** The specific leaf weight (SLW; on a dry weight basis) of young, fully-expanded *Cannabis*
359   *sativa* L. 'Stillwater' leaves in response to the average photosynthetic photon flux density (APPFD),
360   measured on day 35 after initiation of the 12-h photoperiod. Each datum represents one fan leaf from
361   a single plant.
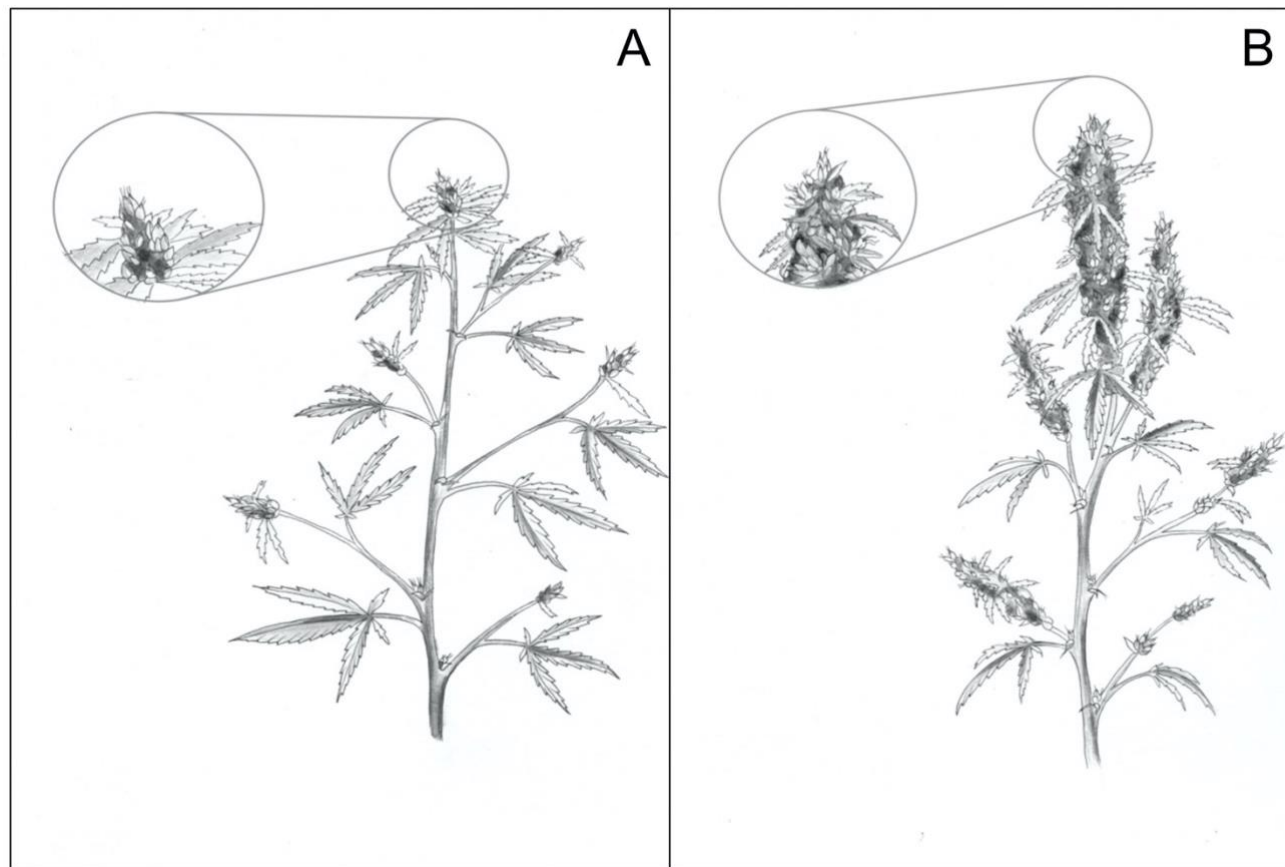
Figure 5. Sketches of *Cannabis sativa* L. 'Stillwater' plants grown under low **(A)** and high **(B)** photosynthetic photon flux density (APPFD), 9 weeks after initiation of 12-h photoperiod (illustrated by Victoria Rodriguez Morrison).

3.2   Chlorophyll Content Index and Plant Morphology

There were no LI treatment effects on CCI either at the top or bottom of the canopy, however within in each week, the upper canopy CCI were higher than the lower canopy. Additionally, the CCI in the upper and lower canopy was higher in week 1 vs. weeks 5 and 9. The CCI (means ± SE, n = 91) were 67.1 ± 0.80, 55.8 ± 2.2, and 52.0 ± 2.1 in the upper canopy and 46.3 ± 1.1, 31.1 ± 0.86, and 31.5 ± 1.1 in the lower canopy, in weeks 1, 5, and 9 respectively. The SLW increased linearly from 35.4 to 58.1 g·m^{-2} as APPFD (calculated based on the respective plants' accumulated PAR exposures up to day 35 of the flowering stage) increased from 130 to 1990 µmol·m^{-2}·s^{-1} (**Figure 4**). Plants grown under low vs. high APPFD were generally shorter and wider, with thinner stems, larger leaves, and fewer, smaller inflorescences (**Figure 5**).

377
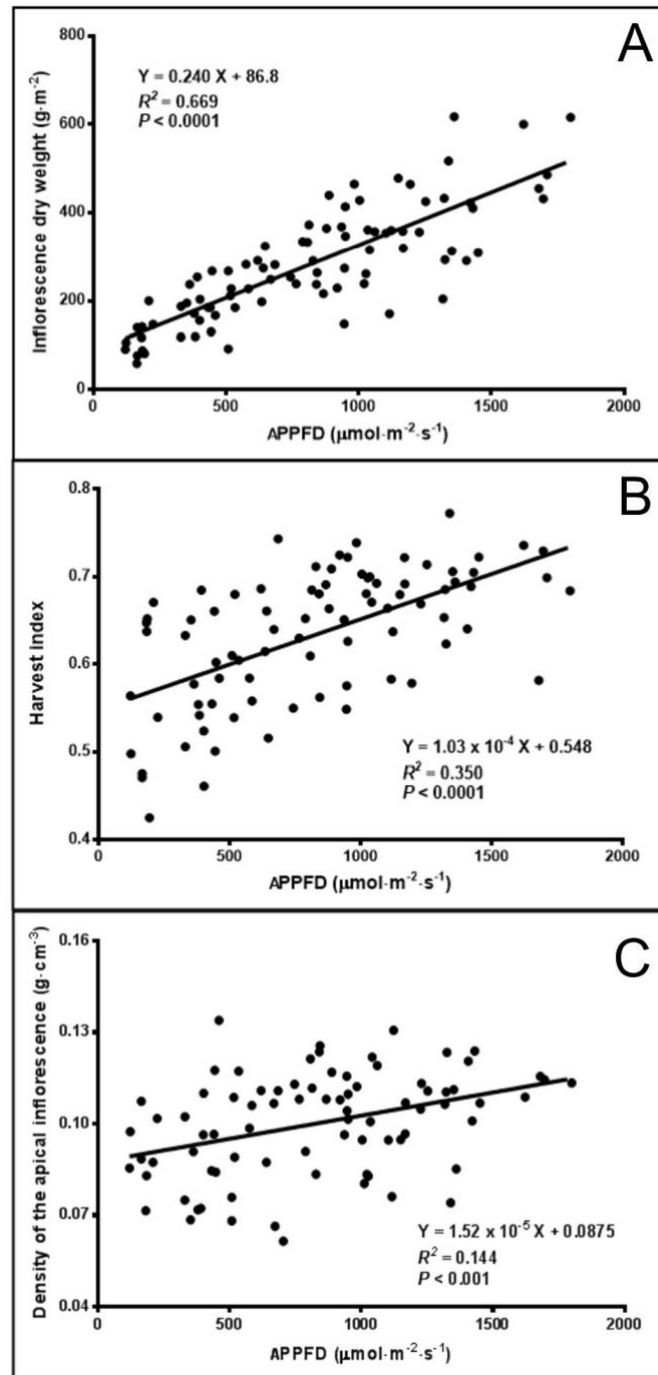
Figure 6. The relationship between average apical photosynthetic photon flux density (APPFD)
applied during the flowering stage (81 days) and inflorescence dry weight **(A)**, harvest index (HI;
total inflorescence dry weight / total aboveground dry weight) **(B)**, and apical inflorescence density
(AID; based on fresh weight) **(C)** of *Cannabis sativa* L. 'Stillwater'. Each datum is a single plant.

Table 1. Cannabinoid potency in apical inflorescences of *Cannabis sativa* L. 'Stillwater'.

Cannabinoid	Potency (mg·g^{-1} of inflorescence dry weight)
Δ-9-tetrahydrocannabinol (Δ^9-THC)	UDL[z]
Δ-9-tetrahydrocannabinolic Acid (Δ^9-THCA)	12.9[y] $\pm$ 0.03
Total equivalent Δ^9-tetrahydrocannabinol (TΔ^9-THC)	11.3 $\pm$ 0.02
Cannabidiol (CBD)	5.53 $\pm$ 0.01
Cannabidiolic acid (CBDA)	214 $\pm$ 0.4
Total equivalent cannabidiol (TCBD)	193 $\pm$ 0.4
Cannabigerol (CBG)	UDL
Cannabigerolic acid (CBGA)	4.76 $\pm$ 0.01
Total equivalent cannabigerol (TCBG)	4.45 $\pm$ 0.009

384 [z]Under detection limit of 0.5 mg·g^{-1} of inflorescence dry weight.
385 [y]Data are means $\pm$ SE (n = 22).
386

387

Table 2. The relationships between average photosynthetic photon flux density (APPFD) applied during the flowering stage (81 days) and terpene potency in apical inflorescences of myrcene, limonene and total terpenes, and the mean potency for terpenes with no APPFD treatment effects, of *Cannabis sativa* L. 'Stillwater'.

Terpene	Terpene potency (mg·g⁻¹ of inflorescence dry weight)		
	Mean [z]	Regression equation [y]	R^2
Total terpenes		Y = 0.00230 X + 8.57	0.320
Myrcene		Y = 0.00142 X + 2.34	0.464
Limonene		Y = 0.000326 X + 1.01	0.246
Alpha pinene	0.16[z] ± 0.01		
Beta pinene	0.22 ± 0.01		
Terpinolene	UDL[x]		
Linalool	0.53 ± 0.01		
Terpineol	0.32 ± 0.02		
Caryophyllene	2.9 ± 0.2		
Humulene	0.65 ± 0.04		
3-carene	UDL		
Cis-ocimene	UDL		
Eucalyptol	UDL		
Trans-ocimene	UDL		
Fenchol	0.22 ± 0.01		
Borneol	0.03 ± 0.01		
Valencene	UDL		
Cis-nerolidol	UDL		
Trans-nerolidol	UDL		
Guaiol	UDL		
Alpha-bisabolol	0.38 ± 0.03		
Sabinene	UDL		

[z]When there were no APPFD treatment effects on terpene potency, the means ± SE (n = 22) are presented.
[y]Linear regression models for the APPFD treatment effects on terpene potency when $P \leq 0.05$.
[x]Under detection limit of 0.5 mg·g⁻¹ of inflorescence dry weight.

397

3.3   Yield and Quality

Cannabis yield increased linearly from 116 to 519 g·m⁻² (i.e., 4.5 times higher) as APPFD increased from 120 to 1800 µmol·m⁻²·s⁻¹ (**Figure 6A**). Note that yields in the present study are true oven-DWs. Since fresh cannabis inflorescences are typically dried to 10 to 15% moisture content to achieve

15

402 optimum marketable quality (Leggett, 2006), yields in the present study can be easily adjusted
403 upwards to be comparable any desirable moisture level (e.g., by multiplying by 1.15 for 15%
404 moisture content). The harvest index increased linearly from 0.560 to 0.733 and (i.e., 1.3 times
405 higher) as APPFD increased from 120 to 1800 µmol·m^{-2}·s^{-1} (**Figure 6B**). The AID increased linearly
406 from 0.0893 to 0.115 g·cm^{-3} (i.e., 1.3 times higher) as APPFD increased from 120 to 1800 µmol·m^{-}
407 ^{2}·s^{-1} (**Figure 6C**).

408 Cannabidiolic acid (CBDA) was the dominant cannabinoid in the dried inflorescences; however,
409 there were no APPFD treatment effects on the potency of any of the measured cannabinoids (**Table**
410 **1**). Due to linear increases in inflorescence yield with increasing LI, cannabinoid yield (g·m^{-2})
411 increased by 4.5 times as APPFD increased from 120 to 1800 µmol·m^{-2}·s^{-1}. Myrcene, limonene, and
412 caryophyllene were the dominant terpenes in the harvested inflorescences (**Table 2**). The potency of
413 total terpenes, myrcene, and limonene increased linearly from 8.85 to 12.7, 2.51 to 4.90, and 1.05 to
414 1.60 mg·g^{-1} inflorescence DW (i.e., 1.4, 2.0 and 1.5 times higher), respectively, as APPFD increased
415 from 120 to 1800 µmol·m^{-2}·s^{-1}. There were no APPFD effects on the potency of the other individual
416 terpenes.

4   DISCUSSION

4.1   Cannabis Inflorescence Yield is Proportional to Light Intensity

419 It was predicted that cannabis yield would exhibit a saturating response to increasing LI, thereby
420 signifying an optimum LI range for indoor cannabis production. However, the yield results of this
421 trial demonstrated cannabis' immense plasticity for exploiting the incident lighting environment by
422 efficiently increasing marketable biomass up to extremely high – for indoor production – LIs (**Figure**
423 **6A**). Even under ambient CO_2, the linear increases in yield indicated that the availability of PAR
424 photons was still limiting whole-canopy photosynthesis at APPFD levels as high as ≈ 1800 µmol·m^{-}
425 ^{2}·s^{-1} (i.e., DLI ≈ 78 mol·m^{-2}·d^{-1}). These results were generally consistent with the trends of other
426 studies reporting linear cannabis yield responses to LI (Eaves et al., 2020; Potter and Duncombe,
427 2012; Vanhove et al., 2011), although there is considerable variability in both relative and absolute
428 yield responses to LI in these prior works. The present study covered a broader range of LI, and with
429 much higher granularity, compared with other similar studies.

430 The lack of a saturating yield response at such high LI is an important distinction between cannabis
431 and other crops grown in controlled environments (Beaman et al., 2009; Fernandes et al., 2013; Oh et
432 al., 2009; Faust, 2003). This also means that the selection of an "optimum" LI for indoor cannabis
433 production can be made somewhat independently from its yield response to LI. Effectively, within
434 the range of practical indoor PPFD levels - the more light that is provided, the proportionally higher
435 the increase in yield will be. Therefore, the question of the optimum LI may be reduced to more
436 practical functions of economics and infrastructure limitations: basically, how much lighting capacity
437 can a grower afford to install and run? This becomes a trade-off between fixed costs which are
438 relatively unaffected by yield and profit (e.g., building lease/ownership costs including property tax,
439 licensing, and administration) and variable costs such as crop inputs (e.g., fertilizer, electricity for
440 lighting) and labor. Variable costs will obviously increase with higher LI but the fixed costs, on a per
441 unit DW basis, should decrease concomitantly with increasing yield (Vanhove et al., 2014). Every
442 production facility will have a unique optimum balance between facility costs and yield; but the yield
443 results in the present study can help cannabis cultivators ascertain the most suitable LI target for their
444 individual circumstances. Readers should be mindful that this study reports yield parameters as true

445   dry weights; marketable yield can be easily determined by factoring back in the desirable moisture
446   content of the inflorescence. For example, for a 400 g·m^{-2} of dry yield, the corresponding marketable
447   yield would be 440 g·m^{-2} at 10% moisture content (i.e., 400 x 1.10).

448   It is also important to appreciate that PPFD, which represents an instantaneous LI level, does not
449   provide a complete accounting of the total photon flux incident on the crop canopy throughout the
450   entire production cycle. While this LI metric is ubiquitous in the horticulture industry and may be
451   most broadly relatable to prior works, there is value in relating yield to the total photon flux received
452   by the crop. Historically, this has been done by relating yield to installed wattage on per area bases,
453   resulting in g·W^{-1} metric (Potter and Duncombe, 2012), which can be more fittingly converted to
454   yield per unit electrical energy input (g·kWh^{-1}) by factoring in the photoperiod and length of the
455   production cycle (EMCDDA, 2013). However, since photosynthesis is considered a quantum
456   phenomenon, crop yield may be more appropriately related to incident (easily measured) or absorbed
457   photons and integrated over the entire production cycle (i.e., TLI, mol·m^{-2}), in a yield metric that is
458   analogous to QY: g·mol^{-1}. Versus using installed wattage, this metric has the advantage of negating
459   the effects of different fixture efficacy (μmol·J^{-1}), which continues its upward trajectory, especially
460   with LEDs (Kusuma et al., 2020; Nelson and Bugbee, 2014). The present study did not directly
461   measure lighting-related energy consumption; however, installed energy flux (kWh·m^{-2}) can be
462   estimated from TLI using the Lumigrow fixture's efficacy rating: 1.29 and 1.80 μmol·J^{-1}, from
463   Nelson and Bugbee (2014) and Radetsky (2018), respectively. Using the average of these values
464   (1.55 μmol·J^{-1}), the conversion from TLI to energy flux becomes: mol·m^{-2} $\times$ 5.6 = kWh·m^{-2}. At an
465   APPFD of 900 μmol·m^{-2}·s^{-1} (i.e., TLI of 3149 mol·m^{-2}), the model in **Figure 6A** predicts a yield of
466   303 g·m^{-2} which corresponds to an energy use efficacy of 0.54 g·kWh^{-1}. For comparison, doubling
467   the LI to the highest APPFD used in this trial increases the yield by 70% but results in a $\approx$ 15%
468   reduction in energy use efficacy. It is up to each grower to determine the optimum balance between
469   variable (e.g., lighting infrastructure and energy costs) and fixed (e.g., production space) costs in
470   selecting a canopy level LI that will maximize profits.

471   **4.2   Increasing Light Intensity Enhances Inflorescence Quality**

472   Beyond simple yield, increasing LI also raised the harvest quality through higher apical inflorescence
473   (also called "chola" in the cannabis industry) density – an important parameter for the whole-bud
474   market – and increased ratios of inflorescence to total aboveground biomass (**Figure 6B and 6C**).
475   The linear increases in HI and AID with increasing LI both indicate shifts in biomass partitioning
476   more in favor of generative tissues; a common response in herbaceous plants (Poorter et al., 2019)
477   including cannabis (Hawley et al., 2018; Potter and Duncombe, 2012). The increases in these
478   attributes under high LI may also indirectly facilitate harvesting, as there is correspondingly less
479   unmarketable biomass to be processed and discarded, which is an especially labour-intensive aspect
480   of cannabis harvesting.

481   The terpene potency – comprised mainly of myrcene, limonene, and caryophyllene – increased by $\approx$
482   25%, as APPFD increased from 130 to 1800 μmol·m^{-2}·s^{-1} (**Table 2**), which could lead to enhanced
483   aromas and higher quality extracts (McPartland and Russo, 2001; Nuutinen, 2018). Conversely, total
484   cannabinoid yield increased in proportion with increasing inflorescence yield since there were no LI
485   treatment effects on cannabinoid potency (**Table 1**). Similarly, Potter and Duncombe (2012) and
486   Vanhove et al. (2011) found no LI treatment effects on cannabinoid potency (primarily THC in those
487   studies) and attributed increasing cannabinoid yield to enhanced biomass apportioning towards
488   generative tissues at higher LI. Other studies had contradictory results on the effects of LI on

17

489   potency. Hawley et al. (2018) did not find canopy position effects on THC or CBD potency in a
490   subcanopy lighting (SCL) trial, but they did find slightly higher cannabigerol potency in the upper
491   canopy in the control (high pressure sodium top-lighting only) and the Red-Green-Blue SCL
492   treatment, but not in the Red-Blue SCL treatment. While it is not possible to unlink spectrum from LI
493   in their results, the magnitude of the reported potency differences, both between canopy positions and
494   between lighting treatments, were relatively minor. Conversely, Namdar et al. (2018) reported what
495   appeared to be a vertical stratification on cannabis secondary metabolites, with highest potencies
496   generally found in the most distal inflorescences (i.e., closest to the light source, PPFD ≈ 600
497    $\mu mol \cdot m^{-2} \cdot s^{-1}$). They attributed this stratification to the localized LI at different branch positions,
498   which were reportedly reduced by ≥ 60% at lower branches vs. at the plant apex. However, given the
499   lack of LI treatment effects (over a much broader range of PPFDs) on cannabinoid potency in the
500   present study, it is likely that other factors were acting on higher-order inflorescences, such as
501   delayed maturation and reduced biomass allocation, that reduced potency in these tissues (Diggle,
502   1995; Hemphill et al., 1980).

4.3   Plasticity of Cannabis Leaf Morphology and Physiology Responses to LI and Over Time

504   The objectives of the photosynthesis and leaf morphology investigations in this study were twofold:
505   1) to address the knowledge gap in the relationships between localized cannabis leaf photosynthesis
506   and yield and 2) observe and report changes in physiology as the plant progresses through the
507   flowering ontogeny.

508   General morphological, physiological, and yield responses of plants are well documented across LI
509   gradients ranging from below compensation point to DLIs beyond 60 $mol \cdot m^{-2} \cdot d^{-1}$. Recently, the LI
510   responses of myriad plant attributes were compiled across a tremendous range species, ecotypes and
511   growing environments, and concisely reported them in the excellent review paper by Poorter et al.
512   (2019). The trends in their LI models align well with primary attributes measured in the present
513   study, including morphological parameters such as plant height and internode length (data not
514   shown), SLW (discussed below), and physiological parameters such as F_v/F_m, LNCER (i.e.,
515   photosynthesis at growth light; Phot/A^{GL}), and A_{sat} (i.e., photosynthesis at saturating light; Phot/A^{SL}).
516   In general, cannabis photosynthesis and yield responses to localized LI were linear across the APPFD
517   range of 120 to 1800 $\mu mol \cdot m^{-2} \cdot s^{-1}$. While these results are in agreement with the contemporary
518   literature on cannabis (Bauerle et al., 2020; Chandra et al., 2008; 2015; Eaves et al., 2020; Potter and
519   Duncombe, 2012), we also showed substantial chronological dependencies on leaf photosynthetic
520   indices.

521   By surveying the photosynthetic parameters of the upper cannabis canopy across a broad range of
522   LPPFDs and over multiple timepoints during the generative phase, we saw evidence of both
523   acclimation and early senescence as the crop progressed through its ontogeny. At the beginning of
524   the trial, the plants were abruptly transitioned from a uniform PPFD (425 $\mu mol \cdot m^{-2} \cdot s^{-1}$) and 18-h
525   photoperiod (i.e., 27.5 $mol \cdot m^{-2} \cdot d^{-1}$) and subjected to a much shorter photoperiod (12-h) and an
526   enormous range of LI (120 to 1800 $\mu mol \cdot m^{-2} \cdot s^{-1}$), resulting in DLIs ranging from 5.2 to 78 $mol \cdot m^{-2} \cdot d^{-1}$. Further, on a DLI-basis, approximately 1/3 of the plants were exposed to lower LIs in the
528   flowering vs. vegetative phase (i.e., APPFD < 640 $\mu mol \cdot m^{-2} \cdot s^{-1}$). These sudden transitions in both LI
529   and photoperiod resulted in substantive changes in the plants' lighting environment at the start of the
530   trial, stimulating various morphological and physiological adaptations with differing degrees of
531   plasticity. The leaves measured in week 1 developed and expanded during the prior vegetative phase
532   under a different lighting regimen (LI and photoperiod). The leaves measured in week 5 were

18

533   developed under their respective LPPFDs during a period characterized by slowing vegetative growth
534   and transitioning to flower development. The leaves measured in week 9 would have also developed
535   under their respective LPPFDs, but since cannabis vegetative growth greatly diminishes after the first
536   five weeks in 12-h days (Potter, 2014), these tissues were physiologically much older than the leaves
537   measured in week 5, with concomitant reductions in photosynthetic capacity (Bauerle et al., 2020;
538   Bielczynski et al., 2017).

539   These differences in leaf physiological age, plant ontogeny, and localized lighting environments
540   during leaf expansion vs. measurement resulted in notable temporal variability in leaf-level LI
541   responses. In week 1, there were no LI treatment effects on A_{sat} and the slopes of the LSP, LNCER,
542   and F_v/F_m were shallower in weeks 5 and 9. The comparatively lower LI responses in week 1 were
543   likely due to the reduced adaptive plasticity that mature foliar tissues have vs. leaves that developed
544   under a new lighting regime (Sims and Pearcy, 1992). Further, Y-intercepts for the A_{sat}, LSP, and
545   LNCER models were higher in week 1 than weeks 5 and 9, which may be partly due to the higher LI
546   (amplified by the longer photoperiod) that the leaves developed under, during the latter part of the
547   vegetative phase. Further, the A_{sat}, LSP, and LNCER models in weeks 5 and 9 have comparable
548   slopes, but there is a vertical translation in the respective models, resulting week 9 models having
549   substantially lower Y-intercepts (i.e., approximately half) for these parameters. The interplay of
550   physiological age of foliage and plant ontogeny (i.e., onset of senescence) on the diminished
551   photosynthetic capacity of the leaves in week 9 is unknown, but the dynamic temporal nature of
552   cannabis photosynthesis (during flowering) is manifest in these models.

553   Given these impacts of physiological age and light history, we posit that cannabis leaf photosynthesis
554   cannot be used as a stand-alone gauge for predicting yield. Chandra et al. (2008) and Chandra et al.
555   (2015) provided insight into the substantial capacity for drug-type strains of indoor grown cannabis
556   leaves to respond to LI; and the results of these trials are much lauded in the industry as evidence that
557   maximum photosynthesis and yields will be reached under canopy-level PPFDs of ≈1500 µmol·m⁻
558   ^{2}·s⁻¹. However, the 400 to 500 µmol·m⁻²·s⁻¹ increments in LPPFD does not provide sufficient
559   granularity (particularly at low LI) to reliably model the LRCs, thus no models were provided.
560   Further, the LRCs were made on leaves of varying and unreported physiological ages, from plants
561   exposed to a vegetative photoperiod (18-h), and acclimated to unspecified localized LI (a canopy-
562   level PPFD of 700 µmol·m⁻²·s⁻¹ was indicated in Chandra et al., 2015). The strong associations
563   between a tissue's light history and its photosynthesis responses to LI, demonstrated in this trial and
564   by others (Björkman, 1981), represent a major shortcoming of using leaf LI response models to infer
565   crop growth and yield. To illustrate, **Figure 2** shows LRCs of leaves from a single cultivar, at similar
566   physiological ages (week 5 after transition to 12-h photoperiod) but acclimated to disparate LPPFDs:
567   91 and 1238 µmol·m⁻²·s⁻¹. The relative difference in LNCER at higher LIs (≈ 50%) between these
568   two curves is representative of the potential uncertainty due to just one of the uncontrolled
569   parameters (LNCER) in these prior works. Differing physiological ages of tissues at the time of
570   measurement may have conferred an even larger degree of uncertainty in the magnitude of leaf
571   responses to LI (Bauerle et al., 2020) than leaf light history. Consideration must also be given to the
572   different life stages of a photoperiodic crop (i.e., vegetative vs. generative) and the inherent impact
573   that day length imbues on the total daily PAR exposure (i.e., DLI) which can correlate better to crop
574   yield than PPFD. Further, for a given DLI, yields are higher under longer photoperiod (Vlahos et al.,
575   1991; Zhang et al., 2018), ostensibly due to their relative proximity to their maximum QY (Ohyama
576   et al., 2005). A final distinction between leaf photosynthesis and whole plant yield responses to LI is
577   the saturating LI: the LSP for leaf photosynthesis were substantially lower than the LSP for yield,
578   which remains undefined due to the linearity of the light response model.

579   Newly-expanded leaves, especially in herbaceous species, are able to vary their leaf size, thickness
580   and chlorophyll content in response to LPPFD in order to balance myriad factors such as internal and
581   leaf surface gas exchange (CO_2 and H_2O), internal architecture of the light-harvesting complexes, and
582   resistance to photoinhibition (Björkman, 1981). In the present study, the effects of LI on leaf
583   morphology was only evaluated in week 5, when the crop was still actively growing vegetative
584   biomass. Reductions in SLW (i.e., increases in specific leaf area, SLA) in response to increasing LI
585   are abundant in the literature (Fernandes et al., 2013; Gratani, 2014; Sims and Pearcy, 1992). In
586   particular, Poorter et al. (2019) reported a saturating response of SLW [also known as leaf mass (per)
587   area; LMA] to LI across 520 species (36% of which were herbaceous plants), however much of their
588   data was at DLIs lower than the minimum DLI in the present study (5.2 mol·m^{-2}·d^{-1}), which affected
589   the shape of their SLW response model to LI. Across similar DLI ranges, the average increase in
590   SLW across 520 species was 1.7 X in Poorter et al., (2019) vs 1.6 X in the present study, indicating
591   that cannabis SLW responses to LI are consistent with normal trends for this parameter.

592   The lack of LI treatment effects on CCI are also consistent with other studies that have shown that
593   area-based chlorophyll content is fairly stable across a broad range of LIs (Poorter et al., 2019;
594   Björkman, 1981), despite substantial variability in photosynthetic efficiency. However, since there
595   were LI treatment effects on SLW, chlorophyll content on leaf volume or mass bases would likely
596   have reduced under higher LI. The positional effects on CCI (i.e., higher in upper vs. lower canopy)
597   were probably due to the interplay between self-shading and advancing physiological age of the
598   lower leaves (Bauerle et al., 2020). The temporal effects on CCI, which was higher in week 1 vs.
599   weeks 5 and 9, in both upper and lower leaves, may have been due to changes in QY over the life-
600   cycle of the crop. Bugbee and Monje (1992) presented a similar trend high QY during the active
601   growth phase of a 60-d crop cycle of wheat, followed by a reduction in QY at the onset of senescence
602   (i.e., shortly before harvest). The decline in chlorophyll content in the latter phase of the production
603   cycle probably contributed to the reductions in the photosynthetic parameters (e.g., A_{sat}, LSP,
604   LNCER) of the tissues measured in week 9 vs. week 5.

605   Overall, the impact that increasing LI had on cannabis morphology and yield were captured
606   holistically in the plant sketches in **Figure 5**, which shows plants grown under higher LIs had shorter
607   internodes, smaller leaves, and much larger and denser inflorescences (resulting in higher HI),
608   especially at the plant apex. Like many other plant species, we have found that cannabis has immense
609   plasticity to rapidly acclimate its morphology and physiology, both at leaf- and whole plant-levels, to
610   changes in the growing lighting environment. Therefore, in order reliably predict cannabis growth
611   and yield to LI, it is necessary to grow plants under a broad range of LIs through their full ontological
612   development, as was done in this study. Without knowing the respective tissues' age and light
613   history, instantaneous light response curves at leaf-, branch-, or even canopy-levels cannot reliably
614   predict yield.

615   **5   CONCLUSIONS**

616   We have shown an immense plasticity for cannabis to respond to increasing LI; in terms of
617   morphology, physiology (over time), and yield. The temporal dynamics in cannabis leaf acclimations
618   to LI have also been explored, addressing some knowledge-gaps in relating cannabis photosynthesis
619   to yield. The results also indicate that the relationship between LI and cannabis yield does not
620   saturate within the practical limits of LI used in indoor production. Increasing LI also increased HI
621   and the size and density of the apical inflorescence; both markers for increasing quality. However,
622   there were no and minor LI treatment effects on potency of cannabinoids and terpenes, respectively.

623 This means that growers may be able to vastly increase yields by increasing LI but maintain a
624 relatively consistent secondary metabolite profile in their marketable products. Ultimately, the
625 selection of the economic optimum canopy-level LI for a given commercial production system
626 depends on many interrelated factors.

627 Future research should expand to multiple cultivars of both indica- and sativa-dominant biotypes.
628 Further, since plant yield responses to elevated CO_2 can mirror the responses to elevated LI, the
629 combined effects of CO_2 and LI should be investigated on cannabis yield with an in-depth cost-
630 benefit analysis of the optimum combination of these two input parameters.

6   ABBREVIATIONS

632 NCER; Net CO_2 exchange rate, PPFD; photosynthetic photon flux, A_{sat}; light-saturated NCER, LSP;
633 light saturation point, QY; maximum quantum yield, CCI; chlorophyll content index, SLW; specific
634 leaf weight, LED; light emitting diode, DLI; daily light integral, PAR; photosynthetically active
635 radiation, DW; dry weight, SD; standard deviation, SE; standard error, RH; relative humidity, Δ^9-
636 THC; Δ-9-tetrahydrocannabinol, Δ^9-THCA; Δ-9-tetrahydrocannabinolic acid, $T\Delta^9$-THC; total
637 equivalent Δ^9-tetrahydrocannabinol, CBD; cannabidiol, TCBD; total equivalent cannabidiol, CBG;
638 cannabigerol, CBGA; cannabigerolic acid, TCBG; total equivalent cannabigerol.

6.1   Non-Standard Abbreviations

640 LPPFD; localized PPFD at the measured leaf, APPFD; average PPFD at the plant apex integrated over
641 time, LNCER; NCER at LPPFD, AID; apical inflorescence density, LI; light intensity, HI; harvest
642 index, TLI; total light integral, LRC; light response curve, CB; deep-water culture basin, UDL; under
643 detection limit

7   AUTHOR CONTRIBUTIONS

8   FUNDING

9   ACKNOWLEDGEMENTS

10   CONTRIBUTION TO THE FIELD STATEMENT

655 *Recent legalization of cannabis in many regions world-wide has provoked demand for scientific*
656 *research to improve cannabis production. Several studies have established models to estimate*
657 *cannabis floral yield response to light intensity. While these works have shown cannabis' immense*
658 *capacity for converting light into marketable biomass, their models cannot be directly utilized by*

659 *cannabis producers without copious assumptions. Therefore, we evaluate the impact of a refined*
660 *range of light intensities (testing the lower and upper limits of practical light intensities used in*
661 *cannabis production) on cannabis physiology, morphology, yield, and quality. We demonstrate the*
662 *extraordinary plasticity of cannabis' physiological, morphological and yield responses to increasing*
663 *light intensity. We also demonstrate that leaf-level photosynthetic responses to light intensity vary*
664 *substantially with leaf age and light history. Therefore, leaf- and plant-level photosynthetic responses*
665 *cannot reliably predict cannabis yield responses to light intensity. This research will assist growers*
666 *in making informed decisions about the optimum light intensity to use for their production systems.*

667

11   REFERENCES

669 Backer, R., Schwinghamer, T., Rosenbaum, P., McCarty, V., Eichhorn Bilodeau, S., Lyu, D.,
670   Ahmed, M.B., Robinson, G., Lefsrud, M., Wilkins, O., Smith, D.L. (2019). Closing the yield
671   gap for cannabis: A meta-analysis of factors determining cannabis yield. Front. Plant Sci.
672   10:495. doi: 10.3389/fpls.2019.00495.

673

674 Bauerle, W.L., McCullough, C., Iversen, M., Hazlett, M. (2020). Leaf age and position effects on
675   quantum yield and photosynthetic capacity in hemp crowns. Plants 9:271. doi:
676   10.3390/plants9020271.

677

678 Beaman, A.R., Gladon, R.J., Schrader, J.A. (2009). Sweet basil requires an irradiance of 500
679   μmol·m^{-2}·s^{-1} for greatest edible biomass production. HortScience 44:64–67. doi:
680   10.21273/HORTSCI.44.1.64.

681

682 Bielczynski, L.W., Łącki, M.K., Hoefnagels, I., Gambin, A., Croce, R. (2017). Leaf and plant age
683   affects photosynthetic performance and photoprotective capacity. Plant Physiol. 175:1634–
684   1648. doi: 10.1104/pp.17.00904.

685

686 Björkman, O. (1981). "Responses to different quantum flux densities," in: Encyclopedia of Plant
687   Physiology: New Series: Vol. 12A, Physiological Plant Ecology 1, eds. L. Lange, P.S. Nobel,
688   C.B. Osmond, and H. Ziegler (Heidelberg, Berlin: Springer-Verlag), 57-107.

689

690 Bredmose, N. (1993). Effects of year-round supplementary lighting on shoot development, flowering
691   and quality of two glasshouse rose cultivars. Sci. Hortic. 54:69–85. doi: 10.1016/0304-
692   4238(93)90084-4.

693

694 Bredmose, N. (1994). Biological efficiency of supplementary lighting on cut roses the year round.
695   Sci. Hortic. 59:75–82. doi: 10.1016/0304-4238(94)90094-9.

696

697 Bugbee, B., Monje, O. (1992). The limits of crop productivity. Bioscience. 42:494–502. doi:
698   10.2307/1311879.

699

700 Carvalho, F.E.L., Ware, M.A., Ruban, A. V. (2015). Quantifying the dynamics of light tolerance in
701   *Arabidopsis* plants during ontogenesis. Plant Cell Environ. 38:2603–2617. doi:
702   10.1111/pce.12574.

703

704   Chandra, S., Lata, H., Khan, I.A., Elsohly, M.A. (2008). Photosynthetic response of *Cannabis sativa*
705   L. to variations in photosynthetic photon flux densities, temperature and CO_2 conditions.
706   Physiol. Mol. Biol. Plants 14:299–306. doi: 10.1007/s12298-008-0027-x.
707
708   Chandra, S., Lata, H., Khan, I.A., ElSohly, M.A. (2011). Photosynthetic response of *Cannabis sativa*
709   L., an important medicinal plant, to elevated levels of CO_2. Physiol. Mol. Biol. Plants
710   17:291–295. doi: 10.1007/s12298-011-0066-6.
711
712   Chandra, S., Lata, H., Mehmedic, Z., Khan, I.A., ElSohly, M.A. (2015). Light dependence of
713   photosynthesis and water vapor exchange characteristics in different high Δ9-THC yielding
714   varieties of *Cannabis sativa* L. J. Appl. Res. Med. Aromat. Plants 2:39–47. doi:
715   10.1016/J.JARMAP.2015.03.002.
716
717   Delgado, E., Parry, M.A.J., Lawlor, D.W., Keys, A.J., Medrano, H. (1993). Photosynthesis, ribulose-
718   1,5-bisphosphate carboxylase and leaf characteristics of *Nicotiana tabacum* L. genotypes
719   selected by survival at low CO_2 concentrations. J. Exp. Bot. 44:1–7. doi: 10.1093/jxb/44.1.1.
720
721   Diggle, P.K. (1995). Architectural effects and the interpretation of patterns of fruit and seed
722   development. Annu. Rev. Ecol. Syst. 26:531–552. doi:
723   10.1146/annurev.es.26.110195.002531.
724
725   Eaves, J., Eaves, S., Morphy, C., Murray, C. (2020). The relationship between light intensity,
726   cannabis yields, and profitability. Agron. J. 112:1466–1470. doi: 10.2139/ssrn.3310456.
727
728   European Monitoring Centre for Drugs and Drug Addiction. (2013). *Cannabis Production and*
729   *Markets In Europe*. Lisbon, Portugal: EMCDDA Insights, No. 12.
730
731   Evergreen Economics. (2016). *Cannabis Agriculture Energy Demand Study Final Report*. San
732   Diego, CA: San Diego Gas & Electric Company.
733
734   Faust, J.E. (2003). "Light," in Ball Redbook, ed. D. Hamrick (Batabia, IL: Ball Publishing), 71–84.
735
736   Fernandes, V.F., de Almeida, L.B., da Feijó, E.V.R.S., da Silva, D.C., de Oliveira, R.A., Mielke,
737   M.S., do Costa, L.C.B. (2013). Light intensity on growth, leaf micromorphology and essential
738   oil production of *Ocimum gratissimum*. Brazilian J. Pharmacogn. 23:419–424. doi:
739   10.1590/S0102-695X2013005000041.
740
741   Gratani, L. (2014). Plant phenotypic plasticity in response to environmental factors. Adv. Bot.
742   2014:1–17. doi: 10.1155/2014/208747.
743
744   Hawley, D., Graham, T., Stasiak, M., Dixon, M. (2018). Improving cannabis bud quality and yield
745   with subcanopy lighting. HortScience 53:1593–1599. doi: 10.21273/hortsci13173-18.
746
747   Hemphill, J.K., Turner, J.C., Mahlberg, P.G. (1980). Cannabinoid content of individual plant organs
748   from different geographical strains of *Cannabis sativa* L. J. Nat. Prod. 43:112–122. doi:
749   10.1021/np50007a009.
750
751   Jones-Baumgardt, C., Llewellyn, D., Ying, Q., Zheng, Y. (2019). Intensity of sole-source light-

752   emitting diodes affects growth, yield, and quality of Brassicaceae microgreens. HortScience.
753   54:1168–1174. doi: 10.21273/HORTSCI13788-18.
754
755   Kirschbaum, M.U.F. (2011). Does enhanced photosynthesis enhance growth? Lessons learned from
756   CO_2 enrichment studies. Plant Physiol. 155:117–124. doi: 10.1104/pp.110.166819.
757
758   Kreyling, J., Schweiger, A.H., Bahn, M., Ineson, P., Migliavacca, M., Morel-Journel, T.,
759   Christiansen, J.R., Schtickzelle, N., Larsen, K.S. (2018). To replicate, or not to replicate - that
760   is the question: How to tackle nonlinear responses in ecological experiments. Ecol. Lett.
761   21:1629–1638. doi: 10.1111/ele.13134.
762
763   Kusuma, P., Pattison, P.M., Bugbee, B. (2020). From physics to fixtures to food: Current and
764   potential LED efficacy. Hortic. Res. 7:56. doi: 10.1038/s41438-020-0283-7.
765
766   Leggett, T. (2006). A review of the world cannabis situation. Bull. Narc. 58: 1–155.
767
768   Lobo, F. A., de Barros, M.P., Dalmagro, H.J., Dalmolin, Â.C., Pereira, W.E., de Souza, É.C.,
769   Vourlitis, G.L., Rodríguez Ortíz, C.E. (2013). Fitting net photosynthetic light-response curves
770   with Microsoft Excel - a critical look at the models. Photosynthetica. 51:445–456. doi:
771   10.1007/s11099-013-0045-y.
772
773   Lydon, J., Teramura, A.H., Coffman, C.B. (1987). UV-B radiation effects on photosynthesis, growth
774   and cannabinoid production of two *Cannabis sativa* chemotypes. Photochem. Photobiol.
775   46:201–206. doi: 10.1111/j.1751-1097.1987.tb04757.x.
776
777   Marcelis, L.F.M., Broekhuijsen, A.G.M., Meinen, E., Nijs, E.M.F.M., Raaphorst, M.G.M. (2006).
778   Quantification of the growth response to light quantity of greenhouse grown crops. Acta
779   Hortic. 711:97–103. doi: 10.17660/actahortic.2006.711.9.
780
781   McPartland, J.M. (2018). *Cannabis* systematics at the levels of family, genus, and species. Cannabis
782   Cannabinoid Res. 3:203–212. doi: 10.1089/can.2018.0039.
783
784   Mills, E. (2012). The carbon footprint of indoor Cannabis production. Energy Policy. 46: 58–67. doi:
785   10.1016/J.ENPOL.2012.03.023.
786
787   Murchie, E., Hubbart, S., Chen, Y., Peng, S., Horton, P. (2002). Acclimation of rice photosynthesis
788   to irradiance under field conditions. Plant Physiol. 130:1999–2010. doi: 10.1104/pp.011098.
789
790   Murchie, E., Lawson, T. (2013). Chlorophyll fluorescence analysis: A guide to good practice and
791   understanding some new applications. J. Exp. Bot. 64:3983–3998. doi: 10.1093/jxb/ert208.
792
793   Namdar, D., Mazuz, M., Ion, A., Koltai, H. (2018). Variation in the compositions of cannabinoid and
794   terpenoids in *Cannabis sativa* derived from inflorescence position along the stem and
795   extraction methods. Ind. Crops Prod. 113:376–382. doi: 10.1016/j.indcrop.2018.01.060.
796
797   Nelson, J.A., Bugbee, B. (2014). Economic analysis of greenhouse lighting: Light emitting diodes vs.
798   high intensity discharge fixtures. PLoS One. 9(6). doi: 10.1371/journal.pone.0099010.
799

800   Niinemets, Ü., Keenan, T.F. (2012). Measures of light in studies on light-driven plant plasticity in
801   artificial environments. Front. Plant Sci. 3:156. doi: 10.3389/fpls.2012.00156.
802
803   Nuutinen, T. (2018). Medicinal properties of terpenes found in *Cannabis sativa* and *Humulus*
804   *lupulus*. Eur. J. Med. Chem. 157:198–228. doi: 10.1016/j.ejmech.2018.07.076.
805
806   Oh, W., Cheon, H., Kim, K.S., Runkle, E.S. (2009). Photosynthetic daily light integral influences
807   flowering time and crop characteristics of *Cyclamen persicum*. HortScience. 44:341–344. doi:
808   10.21273/HORTSCI.44.2.341.
809
810   Ohyama, K., Manabe, K., Omura, Y., Kozai, T., Kubota, C. (2005). Potential use of a 24-hour
811   photoperiod (continuous light) with alternating air temperature for production of tomato plug
812   transplants in a closed system. HortScience. 40:374–377. doi: 10.21273/HORTSCI.40.2.374.
813
814   Poorter, H., Niinemets, Ü., Ntagkas, N., Siebenkäs, A., Mäenpää, M., Matsubara, S., Pons, T. (2019).
815   A meta-analysis of plant responses to light intensity for 70 traits ranging from molecules to
816   whole plant performance. New Phytol. 223:1073–1105. doi: 10.1111/nph.15754.
817
818   Posada, J.M., Sievänen, R., Messier, C., Perttunen, J., Nikinmaa, E., Lechowicz, M.J. (2012).
819   Contributions of leaf photosynthetic capacity, leaf angle and self-shading to the maximization
820   of net photosynthesis in *Acer saccharum*: a modelling assessment. Ann. Bot. 110:731–741.
821   doi: 10.1093/aob/mcs106.
822
823   Potter, D.J. (2014). A review of the cultivation and processing of cannabis (*Cannabis sativa L.*) for
824   production of prescription medicines in the UK. Drug Test. Anal. 6:31–38. doi:
825   10.1002/dta.1531.
826
827   Potter, D.J., Duncombe, P. (2012). The effect of electrical lighting power and irradiance on indoor-
828   grown cannabis potency and yield. J. Forensic Sci. 57:618–622. doi: 10.1111/j.1556-
829   4029.2011.02024.x.
830
831   Radetsky, L.C. (2018). *LED and HID Horticultural Luminaire Testing Report Prepared For Lighting*
832   *Energy Alliance Members and Natural Resources Canada.* Troy, NY: Rensselaer Polytechnic
833   Institute.
834
835   Sen, A., Wyonch, R. (2018). *Cannabis Countdown: Estimating the Size Of Illegal Markets and Lost*
836   *Tax Revenue Post-Legalization.* Toronto, ON: C.D. Howe Institute.
837
838   Sims, D.A., Pearcy, R.W. (1992). Response of leaf anatomy and photosynthetic capacity in *Alocasia*
839   *macrorrhiza* (Araceae) to a transfer from low to high light. Am. J. Bot. 79:449-455. doi:
840   10.2307/2445158.
841
842   Singsaas, E.L., Ort, D.R., DeLucia, E.H. (2001). Variation in measured values of photosynthetic
843   quantum yield in ecophysiological studies. Oecologia 128:15–23. doi:
844   10.1007/s004420000624.
845
846   Terashima, I., Hikosaka, K. (1995). Comparative ecophysiology of leaf and canopy photosynthesis.
847   Plant. Cell Environ. 18:1111–1128. doi: 10.1111/j.1365-3040.1995.tb00623.x.

848
849   Toonen, M., Ribot, S., Thissen, J. (2006). Yield of illicit indoor cannabis cultivation in the
850   Netherlands. J. Forensic Sci. 51:1050–1054. doi: 10.1111/j.1556-4029.2006.00228.x.
851
852   United Nations Office on Drugs and Crime. (2019). *World Drug Report 2019*. United Nations: New
853   York, NY.
854
855   Vanhove, W., Van Damme, P., Meert, N. (2011). Factors determining yield and quality of illicit
856   indoor cannabis (*Cannabis* spp.) production. Forensic Sci. Int. 212:158–163. doi:
857   10.1016/J.FORSCIINT.2011.06.006.
858
859   Vanhove, W., Surmont, T., Van Damme, P., De Ruyver, B. (2014). Filling in the blanks. An
860   estimation of illicit cannabis growers' profits in Belgium. Int. J. Drug Policy 25:436–443. doi:
861   10.1016/j.drugpo.2014.01.020.
862
863   Vlahos, J.C., Heuvelink, E., Martakis, G.F.P. (1991). A growth analysis study of three *Achimenes*
864   cultivars grown under three light regimes. Sci. Hortic. 46:275–282. doi: 10.1016/0304-
865   4238(91)90050-9.
866
867   Zhang, X., He, D., Niu, G., Yan, Z., Song, J. (2018). Effects of environment lighting on the growth,
868   photosynthesis, and quality of hydroponic lettuce in a plant factory. Int. J. Agric. Biol. Eng.
869   11:33–40. doi: 10.25165/j.ijabe.20181102.3420.
870
871   Zheng, Y. (2020). Soilless production of drug-type Cannabis sativa. Acta Hortic. (In press.).
872
873   Zheng, Y., Blom, T., Dixon, M. (2006). Moving lamps increase leaf photosynthetic capacity but not
874   the growth of potted gerbera. Sci. Hortic. 107:380–385. doi: 10.1016/j.scienta.2005.09.004.
875
876